

Late Pleistocene Palaeo Environment Reconstruction from 3D Seismic data, NW Australia. The ACROSS project - Australasian Research: Origins of Seafaring to Sahul.

Anthony Fogg¹, Justin Dix¹, and Helen Farr¹

¹University of Southampton, UK

November 22, 2022

Abstract

The earliest human migration from Sunda (South-East Asian archipelago) to Sahul (Australia and New Guinea) is still heavily debated with proposed timings between c.65-45kaBP depending on the evidence base and interpretation of the data. As part of the EU funded ACROSS project, focused on the mode and route of early migration in to SAHUL, we are undertaking an integrated interpretative study of the evolving submerged landscapes for the Late Pleistocene of the NW Australian Shelf. Oil and gas industry 3D and 2D seismic data, with some core/borehole data, are being used to determine lowstand palaeo-environments and shoreline positions. This information is informing modelling of ocean tide and current patterns that may have been influenced. The seismic is being interpreted supplemented by using time-slices on relative impedance inverted post-stack data. Layer stripping, seismic geomorphology, sequence boundary and depth analysis are being applied to datasets in the Bonaparte Basin, Kimberley Shelf and Arafura regions of Australia's North-West Shelf area. Interpretation of the seismic data is constrained by dated stratigraphy in shallow cores with lower bounds determined from oil/gas well bores. MIS stages 1-4 are identified, however, the seismic response is a composite of time periods due to varying sedimentation rates, non-depositional hiatuses and minimal vertical seismic travel time covering this interval which limits the analysis to the top 50ms TWT (c. 40-45 m) of events below the seabed. This paper reviews the workflows that have been developed to maximise the fine scale detail that can be recovered for a range of terrestrial and marine environments. Procedures include inverse-Q, impedance inversion, spectral decomposition and time-slicing relative to seabed. High resolution 2D seismic data is also being used to augment and inform the interpretation of the conventional oil/gas 3D seismic data. Data examples will be presented showing the geomorphological characteristics (river channels, avulsions, levees, drainage channels, dunes and near shore carbonate reefs) of the lowstand and transgressive landscapes during this period. The palaeo-reconstructions are now being developed from the interpreted seismic geomorphology for the specific consideration of human seaborne travel.

1. INTRODUCTION

The earliest migration of people from Sunda (South-East Asian archipelago) to Sahul (Australia and New Guinea) is still heavily debated with proposed 65-45kaBP depending on the evidence base and interpretation of the data (e.g. Clarkson et al., 2017). As part of the EU funded ACROSS project, focused on the mode and route of early migration in to Sahul, we are undertaking an integrated interpretative study of the evolving submerged landscapes for the Late Pleistocene of the NW Australian Shelf. Oil and gas industry 2D and 3D seismic data, together with some core/borehole data, are being used to determine lowland palaeo-environments and shoreline positions over the last glacial period MIS 1-5e from approximately 125,000 years BP to present (Figure 1). A key focus is on MIS 4 (71,000-59,000 years BP; De Deckker et al., 2019) with a lowstand period from approximately 68,000-63,000 years BP. This time range is consistent with some of the earliest recorded human archaeology in Australia with optical luminescence dates ranging from 50-60kaBP (Hawkins et al., 2017) and Maloney et al's (2018) suggestion of a time of initial settlement in northern Sahul of ~65kaBP. Although mainland Australia was connected to New Guinea at this time a sea crossing would still have been required of at least 70km (Balme, 2013). Several possible routes are mooted which can be categorised as northern routes from SE Asia to New Guinea or southern routes from Timor to NW Australia (e.g. Balme, 2013 and Kealy et al., 2018). Therefore the seismic study is being used to infer palaeo coastal positions associated with the MIS 4 period and elucidate the possible terrestrial and marine landscapes that were present during that period. In turn, the palaeo coastline models will be used to run simulations of tidal and ocean currents to inform possible sea borne transit routes from Sunda to Sahul.

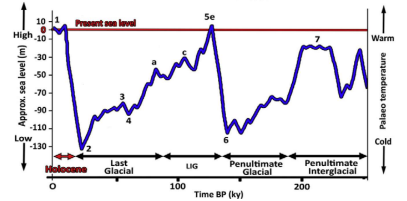


Figure 1. Sea level curve from Benthic et al., 2017 with MIS stages indicated. The Last Glacial Maximum (LGM) corresponds to a lowstand during MIS 2. The MIS 4 lowstand corresponds to the earliest recorded archaeology in Australia. MIS 4 sea level minimum was ~95m compared to present day. MIS 6 is a glacial maximum for the penultimate glacial period - there is a cyclicity to sea level minima.

2. BACKGROUND TO THE SEISMIC DATA ANALYSIS

An extensive 2D and 3D seismic reflection data project database has been created for the NW Australian Shelf centring on the Bonaparte Gulf (Figures 2, 3) using publicly available archives. Interpretation of the seismic data is constrained by dated stratigraphy in shallow cores with lower bounds determined from oil/gas well bores. MIS stages 1-6 are identified within the top 100ms TWT (i.e. 90m) of events below the seabed. High resolution 2D lines are available in the Petrel sub-basin (Figure 2). These lines have proved key in understanding the geomorphology over the past 125,000 years as they allow highstand (thin parallel low energy environment seismic reflection events) and lowstand (incised, chaotic and intra-channel overlapping seismic reflection events) periods to be interpreted. It is possible to interpret highstands associated with MIS 1, MIS 3, MIS 5 and lowstands for MIS 2, MIS 4.

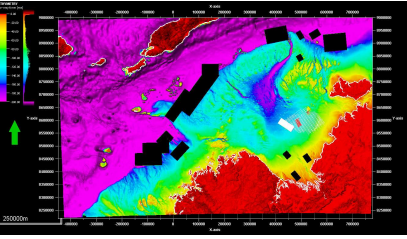


Figure 2. Australia Geoscience 250m bathymetry converted to two-way-time. Contours are denoted by white contours, no red lines present in the Petrel sub-basin. The colored lines represent the 2D seismic coverage for the database used in this study. The white polygons in the Petrel 3D seismic volume in the Petrel sub-basin, white lines are the GAO336 2D survey and red polygons the GAO335 2D high resolution survey.

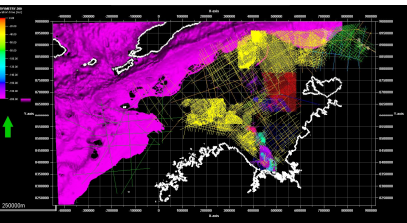


Figure 3. Australia Geoscience 250m bathymetry converted to two-way-time only showing bathymetry >200m (148m). Contours are denoted by white contours. The colored lines represent the 2D seismic coverage for the database used in this study. Additional regional lines are being used, but have been excluded from this image for clarity.

3. INTEGRATING AND ENHANCING THE SEISMIC DATA

The seismic database is multi-vintage necessitating datuming of the different survey acquisition and processing vintages. The Petrel 3D survey has been used as the base survey as it has seven exploration well seabed locations with bathymetry recorded. Seabed picks from the seismic were made at each of the wells, the two-way-time recorded and compared with bathymetry converted to two-way-time using a locally measured wave velocity of 1545m/s (Nicholas et al., 2015). The seismic data was then phase rotated (-30°) to minimise the difference in the two time measurements, differential times reducing from an absolute mean of 1.57ms to 0.57ms. The GAO335 survey high resolution 2D (Jones, 2014) can be tied via the GAO336 survey 2D directly to the Petrel 3D. From this core the area the seismic interpretation has been extended via the network of 2D data, datumed using a seabed pick, to all 3D seismic volumes on the shelf. Minimum processing for 2D and 3D data are depicted by the GREEN process squares below. The ORANGE process squares show the range of other procedures applied to the 3D volumes either as individual or combined procedures.



Figure 4 compares a subline of the Petrel 3D pre and post application of an amplitude only inverse-Q operator (Q=30) optimised using bracketed tests of 20-25-30-35-40. Seismic reflection events are better resolved by the addition of higher frequencies. Four of the 3D datasets have benefited, in terms of near surface interference, from the application of inverse-Q. Higher frequency enhancement can increase apparent noise so some surveys have had a 50m x 50m mean spatial smoother applied to remove high frequency trace to trace variation. Post-stack relative impedance has minimised wavelet sidelobe effects and recovered high frequencies by wavelet removal.

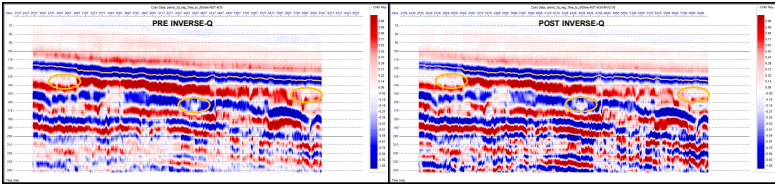
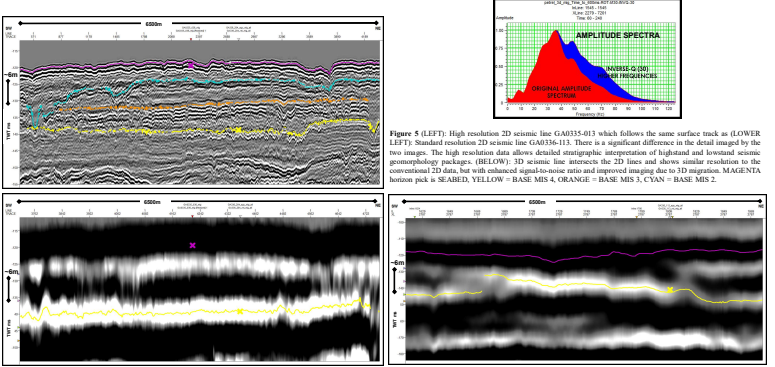


Figure 4 compares a subline of the Petrel 3D (SL1545) pre and post application of an amplitude only inverse-Q operator (Q=30), input seismic has been phase shifted to nominal zero phase at seabed (horizon pick in orange). The inverse-Q increases the resolution between interfacing seismic reflection events in the upper 100ms TWT of the dataset whilst fine scale resolution (see ellipse). The amplitude spectra (BELOW) indicate increase in high frequency content.



4. INTERPRETATION OF SHORELINE AND LANDSCAPE

A process of layer stripping has been used to understand the seismic expression of highstand and lowstand systems in the core analysis area of the Petrel sub-basin. Base MIS 3 and Base MIS 2 have only been picked locally in the Petrel sub-basin.

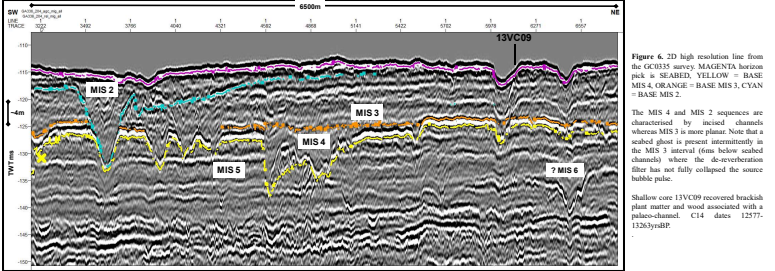


Figure 6. 2D high resolution line from the GAO335 survey. MAGENTA horizon pick is SEABED. YELLOW = BASE MIS 4, ORANGE = BASE MIS 3, CYAN = BASE MIS 2. The MIS 4 and MIS 2 sequences are characterised by incised channels whereas MIS 3 is more planar. Note that a seabed ghost is present intermittently in the MIS 3 interval (omit near seabed channels where the deconvolution filter has not fully corrected the source bubble pulse). Shadow core 13VC09 recovered beach plaster and wood associated with a palaeo-channel. C14 dates 12577-12635aBP. Accounting for subsidence may be important in refining the prediction of emergent land in this region during MIS 4. Courgeon et al (2016) suggest late Quaternary subsidence rates of 0.09m/ka to 0.13m/ka. Using this range 65kaBP would have a subsidence range of 6.2m to 8.8m. Collins (2011) indicates subsidence rates of the order of up to 0.3m/ka for the Kimberley shelf immediately to the south of the Bonaparte Gulf and Bourget et al (2013) propose high subsidence to create accommodation space on the shelf edge. There is uncertainty in terms of what subsidence may be applicable to the Bonaparte Gulf which has implications for what areas might be emergent during MIS 4. MIS 4 can be mapped in to the local vicinity of the Petrel sub-basin, but cannot be continuously mapped across the Bonaparte Gulf. Units attributed to MIS 4 are observed in discrete isolated areas near the shelf edge. Lack of continuity for the Base MIS 4 surface could be due to non-deposition, erosion by later sequences, poor seismic imaging, too thin to image. Two MIS 4 sequence geomorphological features are observed; incised and/or locally thickened units, shore breaks with associated on-lapping sediments. Figure 7 shows the mapped MIS 4 shoreline break and the associated seismic response on conventional 2D data. The shoreline break is seen as a drop seaward in the seabed horizon pick with development of a sediment package to seaward. Clarke and Ringers (2000) interpret strandline (shore faces) in the Holocene for high resolution 2D seismic data in the Bonaparte Gulf by seaward-facing notches and seaward dipping ripples, erosion and beach deposits respectively. This is consistent with the features that have been observed in this study.

4. INTERPRETATION OF SHORELINE AND LANDSCAPE (continued)

Bird et al (2018) use the 75m bathymetric contour as a conservative measure of the minimum area emergent land, but indicate that for 65ka a sea level of 85m would be more appropriate. The mapped shoreline (Figure 7) in this study is consistent with a present day seabed contour of 80m. Figure 8 shows the emergent landscape using the bathymetry contour equivalent to 80m as an indicator. Present day bathymetry therefore appears to be a suitable first order proxy to the MIS 4 shoreline at low stand as the following analysis of the Petrel 3D is consistent with this particular area being estuarine at this period.

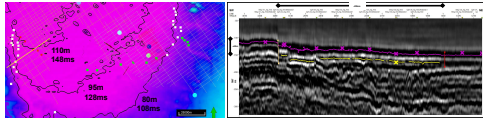


Figure 7. Mapped shore break (white squares) seen at seabed and MIS 4 level based on 2D seismic. Red squares indicate limit of shoreline position given 100ms, 120ms and 140ms TWT contours are shown (corresponding to present day bathymetry of 80m, 95m, 110m). To the east the 100ms contour is a good proxy for the sea with a shallow sloping area. To the west the seabed rises more steeply and the 120ms contour shows a better correspondence. 2D seismic line shows the seaward sediment package (1) developed during the MIS 4 period and markers corresponding to the shoreline break (left) and sediment package (dash) pick (right).

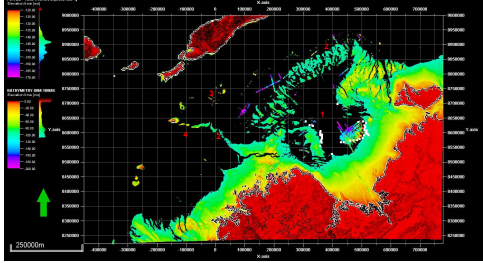


Figure 8. Present day bathymetry showing emergent landscape based on 100ms (80m) contour for the MIS 4 lowstand. Base MIS 4 picks are also displayed, the seismic geomorphology of these events is estuarine or marine. Mapped shore break positions and depositional margins (white circles) also displayed. Present day coastline shown as a black contour. Provisional predicted MIS 4 lowstand emergent landscape using the 80m seabed bathymetry as a proxy indicates the Malta basin (1) is open to the sea with an inner (2) and outer (3) sub-channel and peninsular (4).

Figure 9 (right) shows relative impedance sections flattened relative to seabed. At 4ms there is a dominant SE-NW trending broad channel (A) approximately 3km across. It exhibits multi-phase, high energy flow with evidence of avulsions beyond the channel boundary. This is cross-cut by a later phase low energy narrow channel (B) with a more northerly trend SSE-NNW which is ~300m wide and becomes diffuse to the NW indicating a probable estuarine facies. Field (2018) reports an increase in monsoon activity from ~17kaBP resulting in greater fluvial activity in NW Australia with a possible extreme flood ~10.3kaBP. The broad high energy channel seen here is consistent with increased terrestrial precipitation and associated erosion, but appears to be wholly fluvial, i.e. in an emergent landscape. There are no extant reports of sub-sea turbidite flows in this area so the high energy channel system is interpreted as fluvial. At >20ms the character of channel C is fluvial. However, this channel is a 'sidelobe' 'ghost' to a deeper unit which the post-stack impedance inversion has not fully removed. The >40ms slice shows the channel more clearly as a soft fill cutting in to a broader hard fill channel. This >40ms level is interpreted as the MIS 6 to MIS 5 transition and is comparable with the high energy and low energy phases seen for the MIS 2 to MIS 1 transition (<4ms slice). For the >20ms slice, immediately to the NE of channel C is a group of sub-linear features (D) which may correspond to sand bars or spays (see spectral decomposition slice Figure 10). Broad (>2km) sinuous low energy features are interpreted as estuarine deposits.

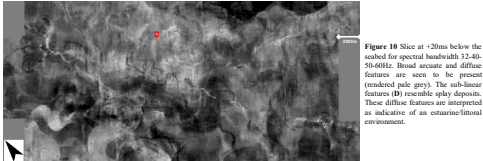


Figure 9 (right) shows relative impedance sections flattened relative to seabed. At 4ms there is a dominant SE-NW trending broad channel (A) approximately 3km across. It exhibits multi-phase, high energy flow with evidence of avulsions beyond the channel boundary. This is cross-cut by a later phase low energy narrow channel (B) with a more northerly trend SSE-NNW which is ~300m wide and becomes diffuse to the NW indicating a probable estuarine facies. Field (2018) reports an increase in monsoon activity from ~17kaBP resulting in greater fluvial activity in NW Australia with a possible extreme flood ~10.3kaBP. The broad high energy channel seen here is consistent with increased terrestrial precipitation and associated erosion, but appears to be wholly fluvial, i.e. in an emergent landscape. There are no extant reports of sub-sea turbidite flows in this area so the high energy channel system is interpreted as fluvial. At >20ms the character of channel C is fluvial. However, this channel is a 'sidelobe' 'ghost' to a deeper unit which the post-stack impedance inversion has not fully removed. The >40ms slice shows the channel more clearly as a soft fill cutting in to a broader hard fill channel. This >40ms level is interpreted as the MIS 6 to MIS 5 transition and is comparable with the high energy and low energy phases seen for the MIS 2 to MIS 1 transition (<4ms slice). For the >20ms slice, immediately to the NE of channel C is a group of sub-linear features (D) which may correspond to sand bars or spays (see spectral decomposition slice Figure 10). Broad (>2km) sinuous low energy features are interpreted as estuarine deposits.

Figure 9 (right) shows relative impedance sections flattened relative to seabed. At 4ms there is a dominant SE-NW trending broad channel (A) approximately 3km across. It exhibits multi-phase, high energy flow with evidence of avulsions beyond the channel boundary. This is cross-cut by a later phase low energy narrow channel (B) with a more northerly trend SSE-NNW which is ~300m wide and becomes diffuse to the NW indicating a probable estuarine facies. Field (2018) reports an increase in monsoon activity from ~17kaBP resulting in greater fluvial activity in NW Australia with a possible extreme flood ~10.3kaBP. The broad high energy channel seen here is consistent with increased terrestrial precipitation and associated erosion, but appears to be wholly fluvial, i.e. in an emergent landscape. There are no extant reports of sub-sea turbidite flows in this area so the high energy channel system is interpreted as fluvial. At >20ms the character of channel C is fluvial. However, this channel is a 'sidelobe' 'ghost' to a deeper unit which the post-stack impedance inversion has not fully removed. The >40ms slice shows the channel more clearly as a soft fill cutting in to a broader hard fill channel. This >40ms level is interpreted as the MIS 6 to MIS 5 transition and is comparable with the high energy and low energy phases seen for the MIS 2 to MIS 1 transition (<4ms slice). For the >20ms slice, immediately to the NE of channel C is a group of sub-linear features (D) which may correspond to sand bars or spays (see spectral decomposition slice Figure 10). Broad (>2km) sinuous low energy features are interpreted as estuarine deposits.

Figure 9 (right) shows relative impedance sections flattened relative to seabed. At 4ms there is a dominant SE-NW trending broad channel (A) approximately 3km across. It exhibits multi-phase, high energy flow with evidence of avulsions beyond the channel boundary. This is cross-cut by a later phase low energy narrow channel (B) with a more northerly trend SSE-NNW which is ~300m wide and becomes diffuse to the NW indicating a probable estuarine facies. Field (2018) reports an increase in monsoon activity from ~17kaBP resulting in greater fluvial activity in NW Australia with a possible extreme flood ~10.3kaBP. The broad high energy channel seen here is consistent with increased terrestrial precipitation and associated erosion, but appears to be wholly fluvial, i.e. in an emergent landscape. There are no extant reports of sub-sea turbidite flows in this area so the high energy channel system is interpreted as fluvial. At >20ms the character of channel C is fluvial. However, this channel is a 'sidelobe' 'ghost' to a deeper unit which the post-stack impedance inversion has not fully removed. The >40ms slice shows the channel more clearly as a soft fill cutting in to a broader hard fill channel. This >40ms level is interpreted as the MIS 6 to MIS 5 transition and is comparable with the high energy and low energy phases seen for the MIS 2 to MIS 1 transition (<4ms slice). For the >20ms slice, immediately to the NE of channel C is a group of sub-linear features (D) which may correspond to sand bars or spays (see spectral decomposition slice Figure 10). Broad (>2km) sinuous low energy features are interpreted as estuarine deposits.

Figure 9 (right) shows relative impedance sections flattened relative to seabed. At 4ms there is a dominant SE-NW trending broad channel (A) approximately 3km across. It exhibits multi-phase, high energy flow with evidence of avulsions beyond the channel boundary. This is cross-cut by a later phase low energy narrow channel (B) with a more northerly trend SSE-NNW which is ~300m wide and becomes diffuse to the NW indicating a probable estuarine facies. Field (2018) reports an increase in monsoon activity from ~17kaBP resulting in greater fluvial activity in NW Australia with a possible extreme flood ~10.3kaBP. The broad high energy channel seen here is consistent with increased terrestrial precipitation and associated erosion, but appears to be wholly fluvial, i.e. in an emergent landscape. There are no extant reports of sub-sea turbidite flows in this area so the high energy channel system is interpreted as fluvial. At >20ms the character of channel C is fluvial. However, this channel is a 'sidelobe' 'ghost' to a deeper unit which the post-stack impedance inversion has not fully removed. The >40ms slice shows the channel more clearly as a soft fill cutting in to a broader hard fill channel. This >40ms level is interpreted as the MIS 6 to MIS 5 transition and is comparable with the high energy and low energy phases seen for the MIS 2 to MIS 1 transition (<4ms slice). For the >20ms slice, immediately to the NE of channel C is a group of sub-linear features (D) which may correspond to sand bars or spays (see spectral decomposition slice Figure 10). Broad (>2km) sinuous low energy features are interpreted as estuarine deposits.

Figure 9 (right) shows relative impedance sections flattened relative to seabed. At 4ms there is a dominant SE-NW trending broad channel (A) approximately 3km across. It exhibits multi-phase, high energy flow with evidence of avulsions beyond the channel boundary. This is cross-cut by a later phase low energy narrow channel (B) with a more northerly trend SSE-NNW which is ~300m wide and becomes diffuse to the NW indicating a probable estuarine facies. Field (2018) reports an increase in monsoon activity from ~17kaBP resulting in greater fluvial activity in NW Australia with a possible extreme flood ~10.3kaBP. The broad high energy channel seen here is consistent with increased terrestrial precipitation and associated erosion, but appears to be wholly fluvial, i.e. in an emergent landscape. There are no extant reports of sub-sea turbidite flows in this area so the high energy channel system is interpreted as fluvial. At >20ms the character of channel C is fluvial. However, this channel is a 'sidelobe' 'ghost' to a deeper unit which the post-stack impedance inversion has not fully removed. The >40ms slice shows the channel more clearly as a soft fill cutting in to a broader hard fill channel. This >40ms level is interpreted as the MIS 6 to MIS 5 transition and is comparable with the high energy and low energy phases seen for the MIS 2 to MIS 1 transition (<4ms slice). For the >20ms slice, immediately to the NE of channel C is a group of sub-linear features (D) which may correspond to sand bars or spays (see spectral decomposition slice Figure 10). Broad (>2km) sinuous low energy features are interpreted as estuarine deposits.

Figure 9 (right) shows relative impedance sections flattened relative to seabed. At 4ms there is a dominant SE-NW trending broad channel (A) approximately 3km across. It exhibits multi-phase, high energy flow with evidence of avulsions beyond the channel boundary. This is cross-cut by a later phase low energy narrow channel (B) with a more northerly trend SSE-NNW which is ~300m wide and becomes diffuse to the NW indicating a probable estuarine facies. Field (2018) reports an increase in monsoon activity from ~17kaBP resulting in greater fluvial activity in NW Australia with a possible extreme flood ~10.3kaBP. The broad high energy channel seen here is consistent with increased terrestrial precipitation and associated erosion, but appears to be wholly fluvial, i.e. in an emergent landscape. There are no extant reports of sub-sea turbidite flows in this area so the high energy channel system is interpreted as fluvial. At >20ms the character of channel C is fluvial. However, this channel is a 'sidelobe' 'ghost' to a deeper unit which the post-stack impedance inversion has not fully removed. The >40ms slice shows the channel more clearly as a soft fill cutting in to a broader hard fill channel. This >40ms level is interpreted as the MIS 6 to MIS 5 transition and is comparable with the high energy and low energy phases seen for the MIS 2 to MIS 1 transition (<4ms slice). For the >20ms slice, immediately to the NE of channel C is a group of sub-linear features (D) which may correspond to sand bars or spays (see spectral decomposition slice Figure 10). Broad (>2km) sinuous low energy features are interpreted as estuarine deposits.

Figure 9 (right) shows relative impedance sections flattened relative to seabed. At 4ms there is a dominant SE-NW trending broad channel (A) approximately 3km across. It exhibits multi-phase, high energy flow with evidence of avulsions beyond the channel boundary. This is cross-cut by a later phase low energy narrow channel (B) with a more northerly trend SSE-NNW which is ~300m wide and becomes diffuse to the NW indicating a probable estuarine facies. Field (2018) reports an increase in monsoon activity from ~17kaBP resulting in greater fluvial activity in NW Australia with a possible extreme flood ~10.3kaBP. The broad high energy channel seen here is consistent with increased terrestrial precipitation and associated erosion, but appears to be wholly fluvial, i.e. in an emergent landscape. There are no extant reports of sub-sea turbidite flows in this area so the high energy channel system is interpreted as fluvial. At >20ms the character of channel C is fluvial. However, this channel is a 'sidelobe' 'ghost' to a deeper unit which the post-stack impedance inversion has not fully removed. The >40ms slice shows the channel more clearly as a soft fill cutting in to a broader hard fill channel. This >40ms level is interpreted as the MIS 6 to MIS 5 transition and is comparable with the high energy and low energy phases seen for the MIS 2 to MIS 1 transition (<4ms slice). For the >20ms slice, immediately to the NE of channel C is a group of sub-linear features (D) which may correspond to sand bars or spays (see spectral decomposition slice Figure 10). Broad (>2km) sinuous low energy features are interpreted as estuarine deposits.

Figure 9 (right) shows relative impedance sections flattened relative to seabed. At 4ms there is a dominant SE-NW trending broad channel (A) approximately 3km across. It exhibits multi-phase, high energy flow with evidence of avulsions beyond the channel boundary. This is cross-cut by a later phase low energy narrow channel (B) with a more northerly trend SSE-NNW which is ~300m wide and becomes diffuse to the NW indicating a probable estuarine facies. Field (2018) reports an increase in monsoon activity from ~17kaBP resulting in greater fluvial activity in NW Australia with a possible extreme flood ~10.3kaBP. The broad high energy channel seen here is consistent with increased terrestrial precipitation and associated erosion, but appears to be wholly fluvial, i.e. in an emergent landscape. There are no extant reports of sub-sea turbidite flows in this area so the high energy channel system is interpreted as fluvial. At >20ms the character of channel C is fluvial. However, this channel is a 'sidelobe' 'ghost' to a deeper unit which the post-stack impedance inversion has not fully removed. The >40ms slice shows the channel more clearly as a soft fill cutting in to a broader hard fill channel. This >40ms level is interpreted as the MIS 6 to MIS 5 transition and is comparable with the high energy and low energy phases seen for the MIS 2 to MIS 1 transition (<4ms slice). For the >20ms slice, immediately to the NE of channel C is a group of sub-linear features (D) which may correspond to sand bars or spays (see spectral decomposition slice Figure 10). Broad (>2km) sinuous low energy features are interpreted as estuarine deposits.

Figure 9 (right) shows relative impedance sections flattened relative to seabed. At 4ms there is a dominant SE-NW trending broad channel (A) approximately 3km across. It exhibits multi-phase, high energy flow with evidence of avulsions beyond the channel boundary. This is cross-cut by a later phase low energy narrow channel (B) with a more northerly trend SSE-NNW which is ~300m wide and becomes diffuse to the NW indicating a probable estuarine facies. Field (2018) reports an increase in monsoon activity from ~17kaBP resulting in greater fluvial activity in NW Australia with a possible extreme flood ~10.3kaBP. The broad high energy channel seen here is consistent with increased terrestrial precipitation and associated erosion, but appears to be wholly fluvial, i.e. in an emergent landscape. There are no extant reports of sub-sea turbidite flows in this area so the high energy channel system is interpreted as fluvial. At >20ms the character of channel C is fluvial. However, this channel is a 'sidelobe' 'ghost' to a deeper unit which the post-stack impedance inversion has not fully removed. The >40ms slice shows the channel more clearly as a soft fill cutting in to a broader hard fill channel. This >40ms level is interpreted as the MIS 6 to MIS 5 transition and is comparable with the high energy and low energy phases seen for the MIS 2 to MIS 1 transition (<4ms slice). For the >20ms slice, immediately to the NE of channel C is a group of sub-linear features (D) which may correspond to sand bars or spays (see spectral decomposition slice Figure 10). Broad (>2km) sinuous low energy features are interpreted as estuarine deposits.

Figure 9 (right) shows relative impedance sections flattened relative to seabed. At 4ms there is a dominant SE-NW trending broad channel (A) approximately 3km across. It exhibits multi-phase, high energy flow with evidence of avulsions beyond the channel boundary. This is cross-cut by a later phase low energy narrow channel (B) with a more northerly trend SSE-NNW which is ~300m wide and becomes diffuse to the NW indicating a probable estuarine facies. Field (2018) reports an increase in monsoon activity from ~17kaBP resulting in greater fluvial activity in NW Australia with a possible extreme flood ~10.3kaBP. The broad high energy channel seen here is consistent with increased terrestrial precipitation and associated erosion, but appears to be wholly fluvial, i.e. in an emergent landscape. There are no extant reports of sub-sea turbidite flows in this area so the high energy channel system is interpreted as fluvial. At >20ms the character of channel C is fluvial. However, this channel is a 'sidelobe' 'ghost' to a deeper unit which the post-stack impedance inversion has not fully removed. The >40ms slice shows the channel more clearly as a soft fill cutting in to a broader hard fill channel. This >40ms level is interpreted as the MIS 6 to MIS 5 transition and is comparable with the high energy and low energy phases seen for the MIS 2 to MIS 1 transition (<4ms slice). For the >20ms slice, immediately to the NE of channel C is a group of sub-linear features (D) which may correspond to sand bars or spays (see spectral decomposition slice Figure 10). Broad (>2km) sinuous low energy features are interpreted as estuarine deposits.

Figure 9 (right) shows relative impedance sections flattened relative to seabed. At 4ms there is a dominant SE-NW trending broad channel (A) approximately 3km across. It exhibits multi-phase, high energy flow with evidence of avulsions beyond the channel boundary. This is cross-cut by a later phase low energy narrow channel (B) with a more northerly trend SSE-NNW which is ~300m wide and becomes diffuse to the NW indicating a probable estuarine facies. Field (2018) reports an increase in monsoon activity from ~17kaBP resulting in greater fluvial activity in NW Australia with a possible extreme flood ~10.3kaBP. The broad high energy channel seen here is consistent with increased terrestrial precipitation and associated erosion, but appears to be wholly fluvial, i.e. in an emergent landscape. There are no extant reports of sub-sea turbidite flows in this area so the high energy channel system is interpreted as fluvial. At >20ms the character of channel C is fluvial. However, this channel is a 'sidelobe' 'ghost' to a deeper unit which the post-stack impedance inversion has not fully removed. The >40ms slice shows the channel more clearly as a soft fill cutting in to a broader hard fill channel. This >40ms level is interpreted as the MIS 6 to MIS 5 transition and is comparable with the high energy and low energy phases seen for the MIS 2 to MIS 1 transition (<4ms slice). For the >20ms slice, immediately to the NE of channel C is a group of sub-linear features (D) which may correspond to sand bars or spays (see spectral decomposition slice Figure 10). Broad (>2km) sinuous low energy features are interpreted as estuarine deposits.

Figure 9 (right) shows relative impedance sections flattened relative to seabed. At 4ms there is a dominant SE-NW trending broad channel (A) approximately 3km across. It exhibits multi-phase, high energy flow with evidence of avulsions beyond the channel boundary. This is cross-cut by a later phase low energy narrow channel (B) with a more northerly trend SSE-NNW which is ~300m wide and becomes diffuse to the NW indicating a probable estuarine facies. Field (2018) reports an increase in monsoon activity from ~17kaBP resulting in greater fluvial activity in NW Australia with a possible extreme flood ~10.3kaBP. The broad high energy channel seen here is consistent with increased terrestrial precipitation and associated erosion, but appears to be wholly fluvial, i.e. in an emergent landscape. There are no extant reports of sub-sea turbidite flows in this area so the high energy channel system is interpreted as fluvial. At >20ms the character of channel C is fluvial. However, this channel is a 'sidelobe' 'ghost' to a deeper unit which the post-stack impedance inversion has not fully removed. The >40ms slice shows the channel more clearly as a soft fill cutting in to a broader hard fill channel. This >40ms level is interpreted as the MIS 6 to MIS 5 transition and is comparable with the high energy and low energy phases seen for the MIS 2 to MIS 1 transition (<4ms slice). For the >20ms slice, immediately to the NE of channel C is a group of sub-linear features (D) which may correspond to sand bars or spays (see spectral decomposition slice Figure 10). Broad (>2km) sinuous low energy features are interpreted as estuarine deposits.

Figure 9 (right) shows relative impedance sections flattened relative to seabed. At 4ms there is a dominant SE-NW trending broad channel (A) approximately 3km across. It exhibits multi-phase, high energy flow with evidence of avulsions beyond the channel boundary. This is cross-cut by a later phase low energy narrow channel (B) with a more northerly trend SSE-NNW which is ~300m wide and becomes diffuse to the NW indicating a probable estuarine facies. Field (2018) reports an increase in monsoon activity from ~17kaBP resulting in greater fluvial activity in NW Australia with a possible extreme flood ~10.3kaBP. The broad high energy channel seen here is consistent with increased terrestrial precipitation and associated erosion, but appears to be wholly fluvial, i.e. in an emergent landscape. There are no extant reports of sub-sea turbidite flows in this area so the high energy channel system is interpreted as fluvial. At >20ms the character of channel C is fluvial. However, this channel is a 'sidelobe' 'ghost' to a deeper unit which the post-stack impedance inversion has not fully removed. The >40ms slice shows the channel more clearly as a soft fill cutting in to a broader hard fill channel. This >40ms level is interpreted as the MIS 6 to MIS 5 transition and is comparable with the high energy and low energy phases seen for the MIS 2 to MIS 1 transition (<4ms slice). For the >20ms slice, immediately to the NE of channel C is a group of sub-linear features (D) which may correspond to sand bars or spays (see spectral decomposition slice Figure 10). Broad (>2km) sinuous low energy features are interpreted as estuarine deposits.

Figure 9 (right) shows relative impedance sections flattened relative to seabed. At 4ms there is a dominant SE-NW trending broad channel (A) approximately 3km across. It exhibits multi-phase, high energy flow with evidence of avulsions beyond the channel boundary. This is cross-cut by a later phase low energy narrow channel (B) with a more northerly trend SSE-NNW which is ~300m wide and becomes diffuse to the NW indicating a probable estuarine facies. Field (2018) reports an increase in monsoon activity from ~17kaBP resulting in greater fluvial activity in NW Australia with a possible extreme flood ~10.3kaBP. The broad high energy channel seen here is consistent with increased terrestrial precipitation and associated erosion, but appears to be wholly fluvial, i.e. in an emergent landscape. There are no extant reports of sub-sea turbidite flows in this area so the high energy channel system is interpreted as fluvial. At >20ms the character of channel C is fluvial. However, this channel is a 'sidelobe' 'ghost' to a deeper unit which the post-stack impedance inversion has not fully removed. The >40ms slice shows the channel more clearly as a soft fill cutting in to a broader hard fill channel. This >40ms level is interpreted as the MIS 6 to MIS 5 transition and is comparable with the high energy and low energy phases seen for the MIS 2 to MIS 1 transition (<4ms slice). For the >20ms slice, immediately to the NE of channel C is a group of sub-linear features (D) which may correspond to sand bars or spays (see spectral decomposition slice Figure 10). Broad (>2km) sinuous low energy features are interpreted as estuarine deposits.

Figure 9 (right) shows relative impedance sections flattened relative to seabed. At 4ms there is a dominant SE-NW trending broad channel (A) approximately 3km across. It exhibits multi-phase, high energy flow with evidence of avulsions beyond the channel boundary. This is cross-cut by a later phase low energy narrow channel (B) with a more northerly trend SSE-NNW which is ~300m wide and becomes diffuse to the NW indicating a probable estuarine facies. Field (2018) reports an increase in monsoon activity from ~17kaBP resulting in greater fluvial activity in NW Australia with a possible extreme flood ~10.3kaBP. The broad high energy channel seen here is consistent with increased terrestrial precipitation and associated erosion, but appears to be wholly fluvial, i.e. in an emergent landscape. There are no extant reports of sub-sea turbidite flows in this area so the high energy channel system is interpreted as fluvial. At >20ms the character of channel C is fluvial. However, this channel is a 'sidelobe' 'ghost' to a deeper unit which the post-stack impedance inversion has not fully removed. The >40ms slice shows the channel more clearly as a soft fill cutting in to a broader hard fill channel. This >40ms level is interpreted as the MIS 6 to MIS 5 transition and is comparable with the high energy and low energy phases seen for the MIS 2 to MIS 1 transition (<4ms slice). For the >20ms slice, immediately to the NE of channel C is a group of sub-linear features (D) which may correspond to sand bars or spays (see spectral decomposition slice Figure 10). Broad (>2km) sinuous low energy features are interpreted as estuarine deposits.

Figure 9 (right) shows relative impedance sections flattened relative to seabed. At 4ms there is a dominant SE-NW trending broad channel (A) approximately 3km across. It exhibits multi-phase, high energy flow with evidence of avulsions beyond the channel boundary. This is cross-cut by a later phase low energy narrow channel (B) with a more northerly trend SSE-NNW which is ~300m wide and becomes diffuse to the NW indicating a probable estuarine facies. Field (2018) reports an increase in monsoon activity from ~17kaBP resulting in greater fluvial activity in NW Australia with a possible extreme flood ~10.3kaBP. The broad high energy channel seen here is consistent with increased terrestrial precipitation and associated erosion, but appears to be wholly fluvial, i.e. in an emergent landscape. There are no extant reports of sub-sea turbidite flows in this area so the high energy channel system is interpreted as fluvial. At >20ms the character of channel C is fluvial. However, this channel is a 'sidelobe' 'ghost' to a deeper unit which the post-stack impedance inversion has not fully removed. The >40ms slice shows the channel more clearly as a soft fill cutting in to a broader hard fill channel. This >40ms level is interpreted as the MIS 6 to MIS 5 transition and is comparable with the high energy and low energy phases seen for the MIS 2 to MIS 1 transition (<4ms slice). For the >20ms slice, immediately to the NE of channel C is a group of sub-linear features (D) which may correspond to sand bars or spays (see spectral decomposition slice Figure 10). Broad (>2km) sinuous low energy features are interpreted as estuarine deposits.

Figure 9 (right) shows relative impedance sections flattened relative to seabed. At 4ms there is a dominant SE-NW trending broad channel (A) approximately 3km across. It exhibits multi-phase, high energy flow with evidence of avulsions beyond the channel boundary. This is cross-cut by a later phase low energy narrow channel (B) with a more northerly trend SSE-NNW which is ~300m wide and becomes diffuse to the NW indicating a probable estuarine facies. Field (2018) reports an increase in monsoon activity from ~17kaBP resulting in greater fluvial activity in NW Australia with a possible extreme flood ~10.3kaBP. The broad high energy channel seen here is consistent with increased terrestrial precipitation and associated erosion, but appears to be wholly fluvial, i.e. in an emergent landscape. There are no extant reports of sub-sea turbidite flows in this area so the high energy channel system is interpreted as fluvial. At >20ms the character of channel C is fluv